

^{15}N and ^{31}P Solid-State NMR Investigations on the Orientation of Zervamicin II and Alamethicin in Phosphatidylcholine Membranes[†]

Burkhard Bechinger,^{*,‡} Dmitry A. Skladnev,[§] Andrey Ogrel,[§] Xing Li,^{||} Elena V. Rogozhkina,[§]
Tatyana V. Ovchinnikova,[⊥] Joe D. J. O'Neil,^{||} and Jan Raap[∇]

Max-Planck-Institut für Biochemie, Am Klopferspitz 18A, 82152 Martinsried, Germany, Shemyakin & Ovchinnikov Institute of Bioorganic Chemistry, Ul. Miklukho-Maklaya 16/10, 117997 GSP-7 Moscow V-437, Russian Federation, Lomonosov State Academy of Fine Chemical Technology, Vernadsky prospekt 86, 117571 Moscow, Russian Federation, Department of Chemistry, University of Manitoba, Winnipeg, Canada R3T 2N2, and Leiden Institute of Chemistry, Gorlaeus Laboratories, Leiden University, Einsteinweg 55, P.O. Box 9502, 2300 RA Leiden, The Netherlands

Received January 25, 2001; Revised Manuscript Received April 20, 2001

ABSTRACT: The topologies of zervamicin II and alamethicin, labeled with ^{15}N uniformly, selectively, or specifically, have been investigated by oriented proton-decoupled ^{15}N solid-state NMR spectroscopy. Whereas at lipid-to-peptide (L/P) ratios of 50 (wt/wt) zervamicin II exhibits transmembrane alignments in 1,2-dicapryl (di-C10:0-PC) and 1,2-dilauroyl (di-C12:0-PC) phosphatidylcholine bilayers, it adopts orientations predominantly parallel to the membrane surface when the lengths of the fatty acyl chains are extended. The orientational order of zervamicin II increases with higher phospholipid concentrations, and considerable line narrowing is obtained in di-C10:0-PC/zervamicin II membranes at L/P ratios of 100 (wt/wt). In contrast to zervamicin, alamethicin is transmembrane throughout most, if not all, of its length when reconstituted into 1-palmitoyl-2-oleoyl-*sn*-glycero-3-phosphocholine bilayers. The ^{31}P solid-state NMR spectra of all phospholipid/peptaibol samples investigated show a high degree of headgroup order, indicating that the peptides do not distort the bilayer structure. The observed differences in peptide orientation between zervamicin and alamethicin are discussed with reference to differences in their lengths, helical conformations, distribution of (hydroxy)proline residues, and hydrophobic moments. Possible implications for peptaibol voltage-gating are also described.

Peptaibols are small antibiotic, hydrophobic peptides of fungal origin (reviewed in refs 1–5). Alamethicin, a member of this class of polypeptides, has been thoroughly studied in the past as it is considered a paradigm for channel formation in biological membranes. Structural analysis by X-ray crystallography (6), as well as NMR¹ spectroscopy in methanolic solution (7), and in the presence of SDS micelles (8, 9), indicates that alamethicin adopts predominantly helical

conformations. A flexible hinge region associated with the helix-breaking motif G-X-X-P at glycine-11 (10) results in a less regular helix conformation or considerable conformational averaging of the C-terminal residues (7, 8, 11). These structural findings are in agreement with molecular dynamics simulations (12, 13). In addition, FTIR, Raman, and CD spectroscopies show that the degree of helicity is dependent on the physical state of the lipid (14), the lipid/peptide ratio (15), and the presence of transmembrane potentials (16).

ESR studies on the effect of molecular oxygen and paramagnetic ions on spin-labeled alamethicin indicate that the N-terminus remains 16 Å distant from the headgroup phosphates of the opposing bilayer leaflet when the peptide is inserted perpendicular to the membrane surface (17). It appears that hydrogen-bonding interactions between polar side chains of the C-terminal helix and phospholipid headgroups as well as associated solvent anchor the peptide at the bilayer–water interface (8, 12, 13, 18).

When added to lipid bilayers, the polypeptide exhibits a well-defined pattern of successive increases in conductance levels, each of a duration of a few milliseconds (19, 20). These voltage-dependent conductance changes are similar to those seen in the presence of large voltage- or ligand-gated channel proteins (reviewed in refs 1, 2, and 4). The open alamethicin pore has been suggested to consist of “transmembrane helical bundles” or “barrel staves” (2), a model consistent with the behavior of covalent alamethicin

[†] Part of the work described in this paper was made possible by the Netherlands Organization of Scientific Research (NWO), Project 047.006.009.

* To whom correspondence should be addressed. Phone: +49 89 8578-2466. Fax: +49 89 8578-2876. E-mail: bechinger@biochem.mpg.de.

[‡] Max-Planck-Institut für Biochemie.

[§] Lomonosov State Academy of Fine Chemical Technology.

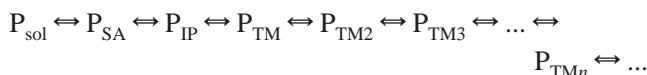
^{||} University of Manitoba.

[⊥] Shemyakin & Ovchinnikov Institute of Bioorganic Chemistry.

[∇] Leiden University.

¹ Abbreviations: di-C10:0-PC, 1,2-dicapryl-*sn*-glycero-3-phosphocholine; di-C12:0-PC, 1,2-dilauroyl-*sn*-glycero-3-phosphocholine; DMPC, 1,2-dimyristoyl-*sn*-glycero-3-phosphocholine (di-C14:0-PC); DOPC, 1,2-dioleoyl-*sn*-glycero-3-phosphocholine (di-C18:1-PC); DPC, dodecyl phosphocholine; ESR, electron spin resonance; FAB MS, fast atom bombardment mass spectrometry; L/P, lipid/peptide; NMR, nuclear magnetic resonance; POPC, 1-palmitoyl-2-oleoyl-*sn*-glycero-3-phosphocholine (C16:0-C18:1-PC); P_{SA}, surface-associated peptide; P_{sol}, soluble peptide; P_{TM}, transmembrane peptide; P_{TMh}, transmembrane helical assemblies consisting of *n* peptides; RP-HPLC, reversed-phase high-performance liquid chromatography; SDS, sodium dodecyl sulfate; TFE, trifluoroethanol; wt, weight.

dimers (21). In the models, the smallest conducting structures consist of trimers (conductivity 19 pS at 1 M KCl (22)) or tetramers (88 pS at 0.5 M KCl (23)), and as many as 20 conductance states probably involving larger aggregates have been observed (24). The interactions of alamethicin with lipid membranes can be described by the following equilibria:



where P_{sol} represents the soluble peptide, P_{SA} indicates the membrane-surface-associated peptide, P_{IP} indicates the membrane-inserted in-plane-oriented peptide, and $P_{\text{TM}n}$ refers to transmembrane helical assemblies consisting of n peptides (5, 25–27). At high lipid-to-peptide ratios the peptides associate with the surface of a membrane; however, above a threshold concentration the peptides form self-associated pores (28). Correspondingly, a minimal peptide concentration is required in the medium for antibiotic activity. The present study focuses on the investigation of $P_{\text{IP}} \leftrightarrow P_{\text{TM}}$ transitions.

Various models for the molecular mechanism of alamethicin voltage-gating are based on interactions of the alamethicin helix dipole with the electric field (reviewed in refs 1, 3, 4, and 29). The dipole moment of alamethicin corresponds to a net +1/2 charge at the N-terminus and a -1/2 charge at the C-terminus of the helix (75 D (30)). Whereas in most of the suggested models voltage-gating involves reorientation of part or all of the helix dipole, it has also been observed that partitioning of alamethicin from solution into the membrane increases with the applied transmembrane voltage (31, 32).

Despite intensive research, our understanding of the detailed mechanism of voltage-dependent channel formation by alamethicin remains incomplete in part because of a paucity of information about the structure of the peptide in a membrane. However, even less is known about the structures and activities of other peptaibols such as zervamicin II, which are considered to form channels by related mechanisms (33–36).

Zervamicin is four amino acids shorter than alamethicin and contains a higher proportion of polar side chains. X-ray crystallographic (34, 37) and NMR structural (38) studies show that the polar side chains contribute to a hydrophilic face of the molecule, resulting in an amphipathic helix (35). When compared to alamethicin, the resulting hydrophobic moment of zervamicin is more pronounced (2). The zervamicin II conformation is similar to that of alamethicin in that a marked helix bend is observed in the center of the peptides (next to hydroxyproline-10 of zervamicin II and proline-14 of alamethicin). Whereas alamethicin carries prolines at positions 2 and 14, both hydroxyprolines and proline are concentrated at the C-terminal half of zervamicin II (positions 10, 13, and 15). The X-ray structures of zervamicin IIB reveal an interesting intermolecular H-bonding interaction between Hyp10 and the Gln11 side chain which has been suggested to stabilize helical bundles in channel models (33, 37).

To gain better insight into the channel-forming properties of the peptaibols, it is necessary to study their structure and dynamics when associated with phospholipid bilayers. Solid-state NMR spectroscopy has been used successfully to investigate the structure, topology, and dynamics of mem-

brane polypeptides (reviewed in ref 39). In particular, proton-decoupled ^{15}N solid-state NMR spectroscopy has been shown to provide direct access to the alignment of helical polypeptides or their orientational distribution under varying physical conditions (5, 39–41). ^{15}N chemical shifts greater than 200 ppm are indicative of transmembrane alignments, whereas values less than 100 ppm are observed for amphipathic peptides oriented along the membrane surface. Chemical shifts and dipolar couplings obtained from oriented membrane samples by proton-decoupled ^{15}N solid-state NMR spectroscopy suggested that the N-terminus of [Ala6- ^{15}N]-alamethicin adopts a transmembrane orientation under the conditions studied (40). More recently, hydrophobic model peptides have been shown to adopt stable transmembrane alignments in oriented phospholipid bilayers provided that the hydrophobic thickness of the membrane matches the hydrophobic length of the polypeptide within considerable tolerance (42). However, peptides that are too short to span the membrane exhibit a predominantly in-plane orientational distribution. Oriented ^{15}N solid-state NMR spectroscopy has also been used to investigate the topological behavior of peptides containing lysine residues. In the presence of one lysine in the center of an otherwise hydrophobic helix, transmembrane orientations are observed. These results indicate that hydrophobic interactions can overcome unfavorable energy contributions that arise from placing a highly polar amino group in the hydrophobic interior of the membrane (43).

In this paper the topological properties of peptaibols as a function of bilayer composition are investigated using oriented ^{15}N solid-state NMR spectroscopy. Alamethicin and zervamicin II have been labeled with ^{15}N uniformly, specifically, or selectively. Thereafter the peptides have been reconstituted into oriented bilayers. A direct comparison of both peptides reveals significant differences in behavior. These are important for our understanding of the functional mechanisms of voltage-gated channel peptides as well as differences in activities between related peptaibols.

MATERIALS AND METHODS

The sequences of the peptides studied are shown in Chart 1. Alamethicin was prepared as described previously and is more than 92% uniformly labeled with ^{15}N (7). Zervamicin labeled uniformly with ^{15}N was prepared in the following manner: The obligate methylotroph *Methylobacillus flagellatum* was grown at 42 °C on the nutrient medium containing per liter Na_2HPO_4 (6 g), KH_2PO_4 (3 g), NaCl (0.5 g), $^{15}\text{NH}_4\text{Cl}$ (1 g), $\text{MgSO}_4 \cdot 7\text{H}_2\text{O}$ (370 mg), CaCl_2 (11 mg), $\text{FeSO}_4 \cdot 7\text{H}_2\text{O}$ (7.4 mg), $\text{ZnSO}_4 \cdot 7\text{H}_2\text{O}$ (1 mg), $\text{MnCl}_2 \cdot 4\text{H}_2\text{O}$ (0.01 mg), $\text{CoCl}_2 \cdot \text{H}_2\text{O}$ (0.74 mg), CuCl_2 (0.25 mg), $\text{NiCl}_2 \cdot \text{H}_2\text{O}$ (0.07 mg), Na_2MoO_4 (0.07 mg), H_3BO_3 (0.64 mg), EDTA (10 mg), and methanol (10 g), and the pH was maintained at 6.7–7.1. Cultivation was carried out in a laboratory-scale fermenter, Bioflo C30 (New Brunswick Scientific Co.), with a 450 mL working volume. Cells were harvested by centrifugation at 10000g for 15 min, resuspended in 0.3 M HCl, autolysed for 24 h at 60 °C, and neutralized with NaOH. Autolysed biomass was used in the medium for growing fungi as a ^{15}N source.

Zervamicin IIB was isolated from *Emericellopsis salmosynnemata*, strain 336, IMI 58330, kindly donated by the

Chart 1: Amino Acid Sequences of Peptides Used in This Investigation^a

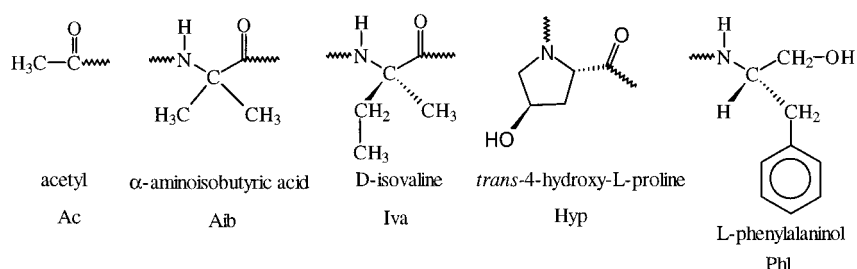
Alamethicin:

Ac Aib Pro Aib Ala Aib Aib **Gln** Aib Val Aib **Gly** Leu Aib Pro Val Aib Aib **Gln Gln Phl**

Zervamicin IIA:

Ac Trp Ile **Gln** Aib Ile **Thr** Aib Leu Aib **Hyp Gln** Aib **Hyp** Aib Pro **Phl**

Zervamicin IIB

Ac Trp Ile **Gln** Iva Ile **Thr** Aib Leu Aib **Hyp Gln** Aib **Hyp** Aib Pro **Phl**^a Polar residues are shown in bold.

Upjohn Co., Kalamazoo, MI. A 10 mL sample of the 96 h seed culture of the fungus was used to inoculate 200 mL of the fermentation medium consisting of ¹⁵N-containing autolysed biomass (7 g/L) instead of bactopectone and yeast extract, with glucose (10 g/L), starch (10 g/L), and calcium carbonate (8 g/L, pH 7.2). The culture was incubated for 7 days at 28 °C on a shaker at 220 rotations/min.

Fermentation broth was filtered through a glass filter. The filter cake which was obtained was triturated with methanol (5 mL/g). The insoluble material was separated by filtration, and the methanolic extract was concentrated to a small volume and then dried in vacuo on a Speed Vac concentrator. The resulting solid was redissolved in 1.5 mL of methanol, and the insoluble residue was removed by centrifugation.

Reversed-phase high-performance liquid chromatography on the Vydac column 208TP54 C8, 300E pore size, 4.6 mm i.d., 250 mm long, 5 μm (Vydac), was used for isolation of ¹⁵N-labeled zervamicin IIB. Separation of zervamicins IIA and IIB was achieved using an eluent of the ternary mixture methanol/acetonitrile/water (67:14:19, v/v) at a flow rate of 0.5 mL/min. The peptaibols were detected by A₂₁₄. The molecular mass of the isolated product was determined by TOF-MALDI mass spectrometry from *m/z* 1880, which corresponds to the calculated mass of the sodium adduct [M + Na]⁺ of uniformly ¹⁵N-labeled zervamicin IIB. The isotope enrichment (96% ± 2%) was determined, and the sample was shown to be pure by 600 MHz solution-state NMR spectroscopy.

[¹⁵N]Aib-labeled zervamicin was prepared by culturing *E. salmosynnemata* (strain 336, IMI 58330) in 250 mL of medium containing 0.5 g of synthetic >98% ¹⁵N-labeled α-aminoisobutyric acid (44), 2.5 g of D-glucose, 2.5 g of Difco bactopectone, 1.0 g of Difco yeast extract, and 2 g calcium carbonate. The culture was grown aerobically for 7 days using a rotary shaker operating at 250 rpm at 28 °C. The product was purified by methanol extraction of the biomass, gel filtration, and RP-HPLC (45). The protocol ensures that pure peptide is obtained but does not resolve the closely related zervamicin IIA and IIB fractions. The ratio of zervamicin IIA to zervamicin IIB (74:26) and the isotope enrichment of Aib (85%) were determined by means of a FAB MS analysis method that has been described by

Ogrel et al. (46). The amide region of the 2-dimensional (¹⁵N-¹H) HSQC 600 MHz NMR spectrum of the labeled compound in a deuterated chloroform/dimethyl sulfoxide mixture (ratio 7:3, v/v) indicates five strong cross-peaks and a single minor peak. The major proton and nitrogen signals for zervamicin IIA/zervamicin IIB (74:26) are 8.16 (144.0), 7.83 (153.3), 8.13 (154.0), 7.69 (149.5), and 8.09 (151.6) ppm (proton chemical shifts are measured relative to that of tetramethylsilane, whereas the nitrogen chemical shifts (in parentheses) are given relative to that of ¹⁵NH₃, using ¹⁵NH₄NO₃ with δ = 22.3 ppm as an external reference standard). These signals are tentatively assigned to amide NH's of Aib residues in zervamicin IIA at positions 14, 12, 9, 7, and 4, respectively, on the basis of the following rationale: Zervamicins IIA and IIB differ in sequence only at position 4 where IIA contains Aib and IIB contains Iva (Chart 1). The shifts corresponding to Aib₁₄, -12, -9, and -7 are similar to those of synthetic zervamicin IIB, which have been assigned previously (46). The additional strong peak at 8.09 (151.6) ppm thus most likely belongs to Aib₄ of zervamicin IIA. The cross-peaks arising from residues 14, 12, and 9 of zervamicin IIA (74%) and zervamicin IIB (26%) overlap, giving rise to the most intense peaks in the spectrum, whereas a less intense peak is observed at 7.63 (149.5) ppm and is attributed to Aib₇ of zervamicin IIB. This signal is slightly shifted upfield (Δδ = 0.06 ppm) relative to the corresponding signal of zervamicin IIA due to the amino acid substitution at position 4 (Chart 1). From both NMR and mass spectrometric analysis we conclude that no scrambling of the label to other N positions has occurred. On the basis of the closely related properties, we assume that there are no major structural differences between zervamicins IIA and IIB.

Zervamicin IIB, specifically labeled at the α-position of glutamine-11 with ¹⁵N, was achieved by the Fmoc-*tert*-butyl strategy in solution using a fragment condensation approach as has been described elsewhere (47). From 600 MHz solution-state NMR spectroscopy the position of the ¹⁵N label was clearly detected, and the isotope enrichment (98% ± 2%) was determined by FAB mass spectrometry.

For solid-state NMR measurements typically 0.75 mg of peptide (uniformly labeled with ¹⁵N) dissolved in trifluoroethanol was mixed with the appropriate amount of diacyl

phosphocholine (Avanti Polar Lipids, Birmingham, AL). Solutions were then spread onto ≤ 30 cover glasses (9×22 mm). Before the glass slides were stacked on top of each other, all organic solvent was removed by exposure to a high vacuum overnight and the membranes were equilibrated at 93% relative humidity. The samples were tightly sealed, inserted into a flat-coil probehead (48), and, if not indicated otherwise (Figure 5C), introduced into the magnet with the bilayer normal aligned parallel to the magnetic field direction.

Proton-decoupled ^{15}N solid-state NMR spectra were recorded using a Bruker AMX400/MSL or DSX 400 wide-bore NMR spectrometer. For signal enhancement a cross polarization MOIST pulse sequence (49) with the following parameters was used: recycle delay 3 s, spin-lock time 1 ms, spectral width 40000 Hz, acquisition time 1.6–3.2 ms, ^1H decoupling strength 35–40 kHz. Typically 10000–20000 transients were collected in the case of uniformly labeled peptides. Up to 94000 scans were accumulated for selectively labeled samples. During measurements the samples were cooled with a stream of air at ambient temperature. An exponential apodization function of 200 Hz was applied before Fourier transformation, and spectra were calibrated with respect to liquid NH_3 using $^{15}\text{NH}_4\text{Cl}$ (41.5 ppm).

Proton-decoupled ^{31}P solid-state NMR spectra were recorded to analyze the orientational distribution of the phospholipids using a Hahn-echo pulse sequence (50). Typically, the ^{31}P 90° pulse was 3 μs , the echo delay 40 μs , and the recycle delay 1.5 s.

RESULTS

Figure 1 shows proton-decoupled ^{15}N solid-state NMR spectra of uniformly labeled zervamicin in oriented diacyl phosphocholine bilayers. The lengths of the fatty acyl chains, and therefore the hydrophobic thicknesses of the membranes, decrease by steps of two methylenes from DOPC (di-C18:1-PC) (Figure 1A) to di-C10:0-PC (Figure 1E). Zervamicin II is composed of 16 amino acids (Chart 1). The ^{15}N chemical shift anisotropy of the 13 amide backbone nitrogens in helical conformations is expected to yield resonances in the range of 65–230 ppm (39), and the two hydroxyprolyl nitrogens and one prolyl nitrogen are expected in the range of 30–230 ppm (51). The two glutamines and one tryptophan should exhibit side chain isotropic chemical shift values of approximately 115 and 84 ppm, respectively (52). When reconstituted into di-C10:0-PC at lipid-to-peptide ratios ≥ 40 (wt/wt),² a predominant peak maximum at 205 ppm is observed, indicating that most backbone amides are in a transmembrane helix (Figure 1E). Additional resonances are resolved at 175, 144, 97, and 52 ppm (Figure 1E). Some of these probably arise from side chains and/or amides undergoing dynamic averaging. Signal intensities below 100 ppm can also derive from immobilized backbone residues, which deviate from transmembrane helical arrangements. Without further information, such as that obtained from selectively labeled resonances, definite assignment of several minor peaks cannot be made.

In general, the spectra in Figure 1 indicate that as the hydrophobic thickness of the membranes is increased much of the ^{15}N signal intensity shifts to the 60–100 ppm region,

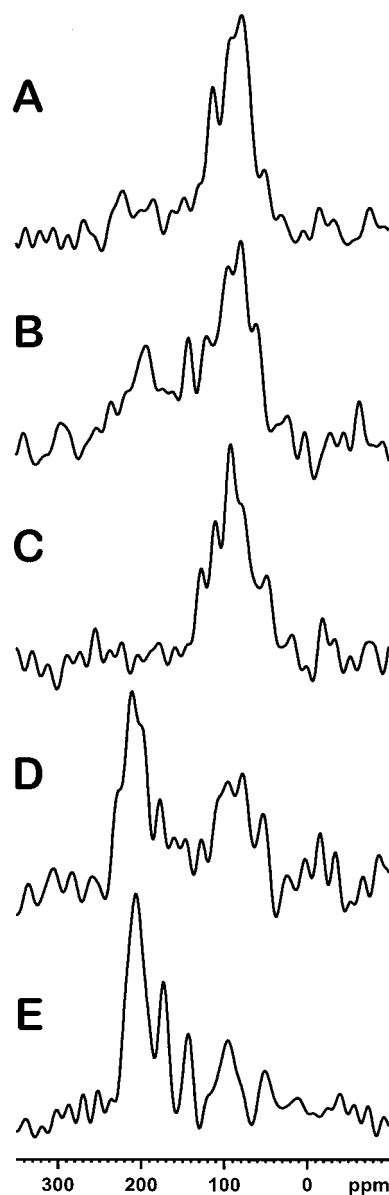


FIGURE 1: Proton-decoupled ^{15}N solid-state NMR spectra of zervamicin II labeled uniformly with ^{15}N and reconstituted into diacyl phosphatidylcholine membranes: (A) DOPC (di-C18:1-PC), (B) di-C16:1-PC, (C) di-C14:1-PC, (D) di-C12:0-PC, (E) di-C10:0-PC. The lipid-to-peptide ratio of all samples is 50 (wt/wt). Sample B was equilibrated at 100% relative humidity, and all others were equilibrated at 93% relative humidity (cf. the text for details). On a molar basis the corresponding L/P ratios are (A) 117, (B) 126, (C) 136, (D) 148, and (E) 162.

suggesting peptide orientations predominantly parallel to the surface of the membrane. In some zervamicin II spectra, including the one obtained in di-C16:1-PC (Figure 1B), the appearance of significant resonance intensities within a broad range of chemical shift anisotropy suggests the presence of randomly oriented peptides (“powder patterns”) and/or peptides in equilibrium between in-plane and transmembrane orientations. Although the ^{15}N solid-state NMR spectra alone are insufficient to differentiate between these two cases, other observations suggest that orientational equilibria are important determinants of the ^{15}N spectra. These include the ^{31}P NMR spectra of the same samples exhibiting a high degree of order of the bilayer phospholipids (Figure 2; cf. below) and the high solubility of zervamicin II in TFE and in membranes. Furthermore, uniform alignments of zervamicins

² Molar ratios are given in the figure captions.

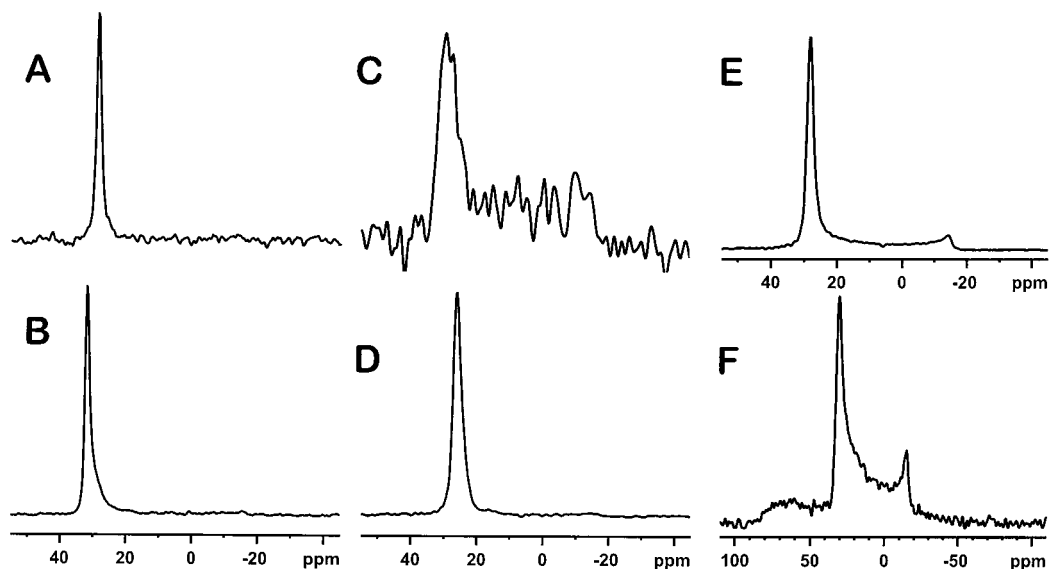


FIGURE 2: Representative proton-decoupled ^{31}P solid-state NMR spectra of oriented di-C10:0-PC (A, B), POPC (C), DOPC (D), di-C14:1-PC (E), or di-C12:0-PC (F) membranes in the presence of zervamicin II. The lipid-to-peptide ratios are (wt/wt) (A) 4, (B) 100, (C) 4.4, and (D–F) 50, or on a molar basis (A) 13, (B) 325, (C) 11, (D) 117, (E) 136, and (F) 148. Please note the different scaling of the axis in (F).

in di-C10:0-PC are obtained when prepared under exactly the same experimental conditions, thereby excluding the possibility of irreversible peptide precipitation during membrane reconstitution (cf. also preparations shown in Figure 4A,B).

To test how zervamicin II affects the order of the phospholipid headgroups, proton-decoupled ^{31}P NMR spectra of oriented zervamicin/lipid mixtures were recorded. A ^{31}P NMR signal at 30 ppm is observed when the long axes of phosphatidylcholines in undistorted liquid crystalline bilayers are oriented parallel to the magnetic field direction (39). Representative proton-decoupled ^{31}P solid-state NMR spectra of the phosphatidylcholine headgroups of samples also investigated by ^{15}N solid-state NMR spectroscopy are shown in Figure 2A–E ($L/P \geq 4$). Parts A and B of Figure 2 indicate that di-C10:0-phosphatidylcholine is well oriented along the surfaces of the cover glasses at lipid-to-peptide ratios of 4 (wt/wt) and 100 (wt/wt). The greatest disorder among the headgroups, judging from the ^{31}P chemical shift dispersion, was observed at low lipid-to-peptide ratios in the presence of POPC (Figure 2C). This spectrum also shows the broadest line width and at constant amounts of peptide in the samples concomitantly the lowest signal-to-noise ratio.

To determine the possible role of variable water activity³ on the ^{15}N spectral line shapes, we acquired ^{15}N NMR spectra of samples between 75% and 100% relative humidity (data not shown). Except for zervamicin in di-C12:0-PC, where relative humidities of <100% reduce the proportion of transmembrane peptide (Figure 1D), the ^{15}N spectral line shapes do not change significantly with changes in relative humidity. However, the ^{31}P NMR spectra of the di-C12:0-PC samples at low hydration also show additional resonance intensities at frequencies >30 ppm, suggesting concomitant phase transitions of the lipid bilayer (Figure 2F).

Parts D and E of Figure 1 indicate that at lipid-to-peptide ratios of 50 (wt/wt) zervamicin II is predominantly oriented in a transmembrane fashion in thin lipid bilayers. However, by increasing the membrane hydrophobic thickness, a predominant orientation perpendicular to the sample normal is observed (Figure 1A–C). To test how peptide alignments are affected by the lipid-to-peptide ratio, additional samples were prepared. In the absence of lipid or in the presence of extremely low lipid concentrations, the zervamicin peptides are oriented in a close to random fashion (Figure 3A,B). Although partial peptide alignment is obtained already at di-C10:0-PC/zervamicin II ratios ≥ 4 (wt/wt) (Figure 3C–E), the lowest orientational disorder (mosaic spread) and, therefore, the smallest resonance line widths are obtained when the amount of di-C10:0-PC is further increased above 40% (wt/wt) (Figure 3F–H).

Zervamicin II labeled at a single site or selected sites was also prepared by chemical or biochemical methods, respectively. Figure 4A shows the ^{15}N solid-state NMR spectrum of zervamicin II labeled at the glutamine-11 backbone site and reconstituted into oriented POPC membranes. The broad distribution of resonances observed even when only a single label is present in the peptide indicates that the molecule adopts a broad range of alignments and/or conformations under these conditions (Figure 4A). The ^{31}P NMR spectra of the same sample show that this orientational distribution occurs with only moderate disturbance of the phospholipid headgroup (not shown). When the peptide/POPC mixture was recovered from the glass plates and diluted with an approximately equal amount of di-C10:0-PC, the resulting POPC/di-C10:0-PC/zervamicin II (50:50:1, wt/wt) mixture yielded a single ^{15}N chemical shift resonance at 187 ppm (Figure 4B). It should be noted that the additional signals observed with biochemically prepared zervamicin (Figures 1E and 3F–H), tentatively assigned to ^{15}N -labeled amino acid side chains, are absent in this preparation.

Similarly [*Aib*_{4/5}- $^{15}\text{N}_{4/5}$]zervamicin II (^{15}N -labeled at several α -aminoisobutyric acid residues: positions (4), 7, 9, 12, and

³ The amount of water that is associated with the membranes is adjusted by equilibrating the samples in a gas phase of defined relative humidity. The vapor pressure of the gas phase is controlled by the composition of saturated salt solutions (71).

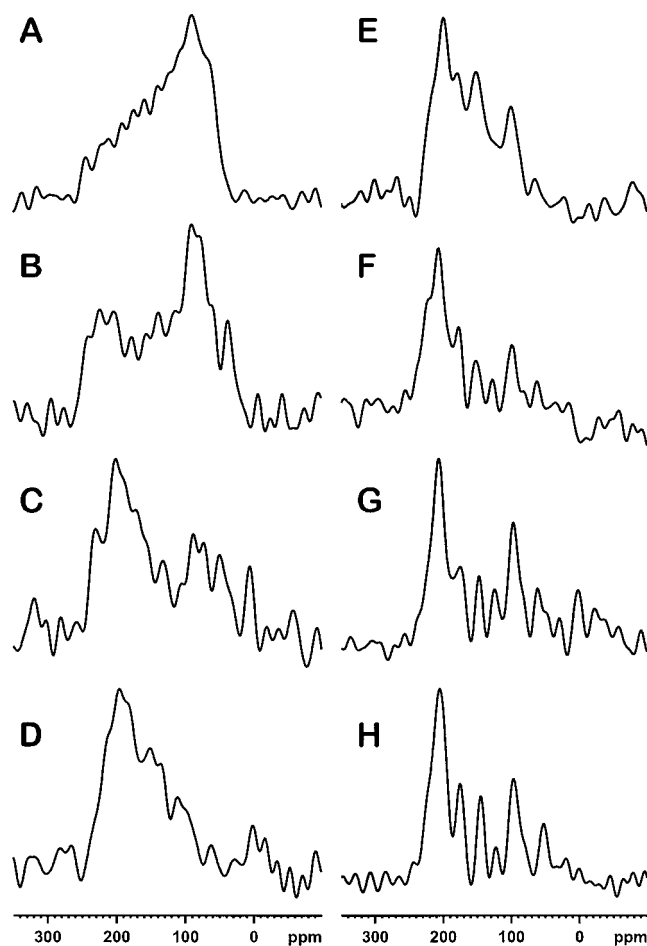


FIGURE 3: Proton-decoupled ^{15}N solid-state NMR spectra of zervamicin II labeled uniformly with ^{15}N and applied to glass plates in the absence of lipids (A), or when reconstituted into oriented di-C10:0-PC membranes at the following lipid-to-peptide ratios (wt/wt): (B) 2, (C) 4, (D) 8, (E) 16, (F) 40, (G) 80, (H) 100. On a molar basis the corresponding L/P ratios are (B) 6.5, (C) 13, (D) 26, (E) 52, (F) 130, (G) 260, and (H) 325.

14; cf. Chart 1) exhibits a broad chemical shift dispersion when reconstituted into POPC membranes (Figure 4C), but predominantly chemical shifts corresponding to a transmembrane alignment (peak maximum at 216 ppm) when reconstituted into di-C10:0-PC (Figure 4D). Figure 4D reveals additional resonance intensities that are also discernible in the spectra of uniformly labeled peptide (Figures 1E and 3F–H). The broad signal with peak maximum at 86 ppm probably reflects peptides oriented perpendicular to the magnetic field direction. Due to the background noise it cannot be unambiguously determined whether the signal intensities between the two main peaks (around 180 and 146 ppm) derive from individual residues or reflect a mosaic spread in transmembrane peptide distributions.

To enable a direct comparison between zervamicin II and alamethicin, uniformly labeled samples of both peptides were incorporated into POPC lipid bilayers at lipid-to-peptide ratios similar to and higher than those used in a previous investigation of $[\text{Ala}6\text{-}^{15}\text{N}]\text{alamethicin}$ (40). POPC was chosen as it represents well the hydrophobic thickness of natural membranes as well as their average saturated/unsaturated fatty acyl chain composition. Also, the bilayer composition is sufficiently close to that used in previous studies (40) to allow for a direct comparison. Most of the

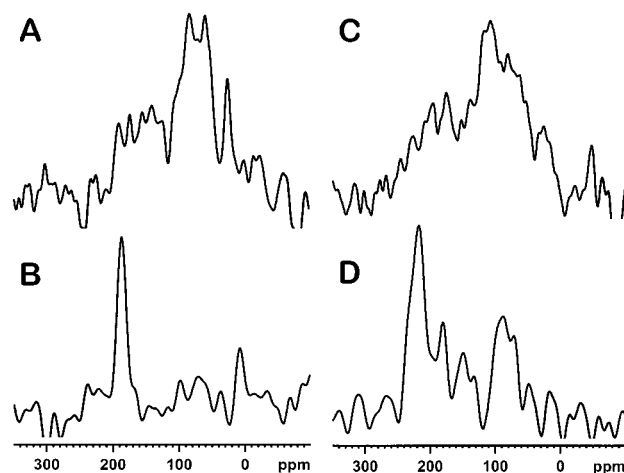


FIGURE 4: Proton-decoupled ^{15}N solid-state NMR spectra of zervamicin labeled at single or selected sites: (A) $[\text{Gln}11\text{-}^{15}\text{N}]\text{-zervamicin II}$ in POPC, L/P = 50 (wt/wt), (B) $[\text{Gln}11\text{-}^{15}\text{N}]\text{-zervamicin II}$ in di-C10:0-PC/POPC ($\sim 1:1$, wt/wt), L/P ≈ 100 (wt/wt), cf. the text for details, (C) $[\text{Aib}_{4/5}\text{-}^{15}\text{N}_{4/5}]\text{zervamicin II}$ in POPC, L/P = 75 (wt/wt), (D) $[\text{Aib}_{4/5}\text{-}^{15}\text{N}_{4/5}]\text{zervamicin II}$ in di-C10:0-PC, L/P = 50 (wt/wt). On a molar basis the corresponding L/P ratios are (A) 120, (B) ~ 275 , (C) 180, and (D) 161. The spectra were recorded by accumulating 33000 (A), 77000 (B), 53000 (C), or 94000 (D) scans.

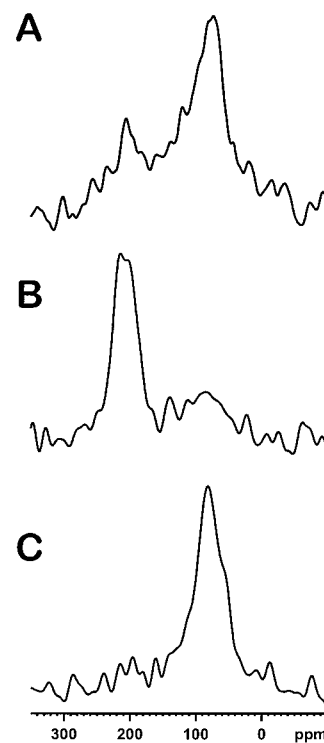


FIGURE 5: Proton-decoupled ^{15}N solid-state NMR spectra of peptaibols labeled uniformly with ^{15}N : (A) zervamicin II in POPC, L/P = 4.4 (wt/wt), (B) alamethicin in POPC, L/P = 5.8 (wt/wt), and (C) alamethicin in POPC, L/P = 90 (wt/wt). The sample normal is perpendicular to the magnetic field direction (i.e., tilted by 90° when compared to (B)). On a molar basis the corresponding L/P ratios are (A) 11, (B) 15, and (C) 237.

alamethicin signal intensity occurs at about 200 ppm (Figure 5B), indicating that the peptide is aligned predominantly in a transmembrane orientation. A 90° tilted alamethicin sample at L/P = 90 (wt/wt) results in ^{15}N chemical shift resonances below 120 ppm (Figure 5C), in agreement with the assignment of the main resonances to peptides belonging to

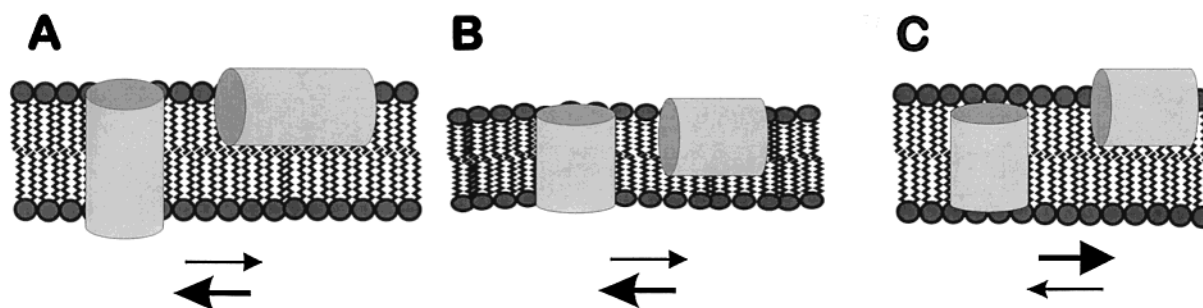


FIGURE 6: Models of in-plane to transmembrane equilibria of (A) alamethicin matching the lipid bilayer thickness, (B) zervamicin II in thin lipid bilayers (hydrophobic mismatch), and (C) a peptide shorter than the hydrophobic thickness of the membrane. Other mechanisms that can compensate for hydrophobic mismatch are discussed in refs 42 and 70. These include conformational changes of lipids and peptides, tilting of peptide helices that exceed the thickness of the bilayer, lipid phase transitions, and peptide association.

molecules with transmembrane alignments of the helix axis (53). In POPC the spectrum of zervamicin (Figure 5A) shows a major component at 75 ppm and a smaller contribution around 207 ppm. Although the appearance of the spectrum exhibits features of a powder pattern that would arise from a random orientation of peptides, for the reasons discussed before (in the context of Figure 1B), the more likely interpretation of this spectrum is that it reflects a dynamic equilibrium between transmembrane (207 ppm) and in-plane (75 ppm) peptides, with the Gibbs free energy of the in-plane state favored by a few kilojoules per mole.

DISCUSSION

Zervamicin II is composed of predominantly hydrophobic amino acids; only about one-quarter are polar, and none of them are charged (Chart 1). The peptide, therefore, strongly interacts with phospholipid membranes. In di-C10:0-PC bilayers predominantly transmembrane alignments are observed at all lipid-to-peptide ratios between 4 and 160 (wt/wt) (Figure 3). However, when the peptide is applied to glass surfaces in the absence of lipids or at L/P = 2 (wt/wt), the solid-state ^{15}N NMR spectra of the peptide resemble powder patterns. This result indicates that interactions of zervamicin II with oriented lipid bilayers are necessary for the peptides' mechanical alignment along glass surfaces at high L/P ratios (Figures 2A,B and 3C–H). As the lipid-to-peptide ratio is increased beyond 4, the peptide orientational dispersion continuously decreases. Once peptide dilutions are reached that would be sufficient for peptides to be well-separated within the lipid bilayer, narrow lines are obtained in proton-decoupled ^{15}N spectra. This suggests that peptide–peptide interactions are not important for obtaining uniform transmembrane alignments but rather that the peptide is oriented by constraints imposed by the ordered lipid bilayer (Figures 3F–H and 4B,D). However, it should be noted that oriented solid-state NMR spectra provide only indirect information on the aggregation state of the peptides (53).

Whereas zervamicin II adopts transmembrane alignments in di-C10:0-PC, it is oriented predominantly parallel to the sample surface when the fatty acyl chains of the bilayer phosphatidylcholines exceed 12 carbon atoms (Figures 1A–C, 4A,C, and 5A). The line shapes of singly or selectively labeled zervamicin II (Figure 4) agree reasonably well with those of uniformly labeled zervamicin II, thereby suggesting that the orientational distribution of the amide bonds is to a large extent determined by the topology of the alignment of the peptide as a whole. Previous investigations show that

hydrophobic model peptides with two lysine anchors at each terminus adopt transmembrane alignments as long as the calculated hydrophobic mismatch⁴ between the peptide and the bilayer does not fall below -3 \AA (peptide too short) or above $+14 \text{ \AA}$ (peptide too long) (42). Helix alignments predominantly parallel to the membrane surface have been observed for peptides that are too short to span the lipid bilayer. These have been described in previous publications by dynamic equilibria (Figure 6) connecting in-plane and transmembrane alignments (27, 42, 43, 54). Both zervamicin II and short model peptides do not significantly disturb the phospholipid headgroup orientation even under conditions where they do not match the hydrophobic thickness of the membrane (Figure 2) (42). This behavior is in contrast with that of model compounds that much exceed the hydrophobic thickness of the lipid bilayer (42).

Although hydrophobic helical model peptides of 16 residues exhibited transmembrane alignments in all phospholipid bilayers tested in a previous investigation (42), zervamicin II only adopts stable transmembrane orientations in bilayers of the shortest fatty acyl chain composition. The estimated hydrophobic length of zervamicin II in a fully extended conformation is only about $18\text{--}20 \text{ \AA}$ (cf. footnote 4). NMR investigations in organic solutions and X-ray crystallographic studies indicate that zervamicin IIB adopts amphipathic helical conformations encompassing all residues (34, 38). The peptide helix exhibits a $40\text{--}50^\circ$ bend at its center. Recent studies indicate that in the presence of DPC micelles very similar conformations of zervamicin II exist, with an orientation of the helix parallel to the micellar interface (A. S. Arseniev, personal communication). Should such a conformation also be maintained in bilayer environments, the length of the zervamicin helix (ca. $15\text{--}17 \text{ \AA}$) indeed falls considerably short of the calculated thickness of 1-palmitoyl-2-oleoylphosphatidylcholine (POPC) and di-C18:1-PC ($26\text{--}27 \text{ \AA}$), di-C16:1-PC (23.5 \AA), di-C14:1-PC, and di-C12:0-PC ($19.5\text{--}20 \text{ \AA}$, cf. Table 2 in ref 42) bilayers.

⁴ The hydrophobic mismatch is calculated from the difference of estimates of the hydrophobic length of the peptide and the thickness of the hydrophobic portion of lipid bilayers. This number only provides an approximate guide line of the true situation. To calculate the length of the peptide, the number of hydrophobic residues was multiplied by 1.5 \AA . As this overestimates the average length of the peptide helix by a half-turn at each terminus (72), 5.4 \AA was subtracted. On the other hand, lysine methylenes at the peptide termini of model peptides can extend the hydrophobic region (42). It should also be noted that the hydrophobic thicknesses of the bilayers used in these calculations are estimates from measuring membrane–membrane spacings.

However, the estimated length of zervamicin II does fit well to the estimated hydrophobic thickness of di-C10:0-PC (15.5 Å). In addition, the peptide exhibits considerable polarity due to several hydroxyl (Thr, Hyp) or carboxamide (Gln) side chains as well as the phenylalaninol terminus (Chart 1). The (hydroxy)proline residues also contribute to the amphipathic character of the helix through non-hydrogen-bonded backbone carbonyl oxygens. We suggest that the amphipathic properties of zervamicin II have a pronounced influence on the peptides' in-plane \leftrightarrow transmembrane equilibria. Whereas hydrophobic interactions keep the peptide inside the membrane, both hydrophobic mismatch and polar energy contributions favor in-plane helical alignments.

It is interesting to compare zervamicin II (16 amino acids) to the 20-residue peptide alamethicin, both belonging to the peptaibol family. The ^{15}N resonances of oriented alamethicin labeled uniformly with ^{15}N indicate transmembrane alignments (Figure 5B,C). Whereas the spectrum shown in Figure 5B is characterized by components close to the σ_{33} value of the static tensor element, the spectrum in Figure 5C exhibits characteristics of σ_{11} and σ_{22} , which are similar in size (39, 53). Good orientation of the alamethicin peptide is obtained even at POPC-to-peptide ratios as low as 4.4 (wt/wt). Inspection of Figure 5B indicates that additional small signal intensities are observed at 50–120 ppm. These are probably due to sample misalignments or a small proportion of peptide that is oriented along the bilayer surface. However, the possibility also exists that a few residues in transbilayer peptides exhibit orientations of their NH vectors parallel to the membrane surface or that side chain intensities contribute. Previously performed oriented ^{15}N solid-state NMR investigations of [Ala6- ^{15}N]alamethicin (40) are consistent with an α -helical conformation and a transmembrane alignment of the N-terminal portion of this peptide. Axially symmetric powder patterns are obtained of this single-site-labeled peptide when it is incorporated into fully hydrated liquid crystalline DMPC membranes, indicating fast reorientation of the Ala6 amide with a single axis of symmetry. The spectrum shown in Figure 5C has been obtained from uniformly labeled peptides at lipid-to-peptide ratios similar to those of the above-mentioned study (40). They indicate that $\geq 75\%$ of the alamethicin residues adopt transmembrane helical alignments. The results shown in Figure 5B,C are also in agreement with previous molecular modeling calculations (25, 55) and oriented CD experiments (56, 57). These latter investigations also indicate that the alignment of alamethicin is governed by the phospholipid composition and phase, membrane hydration, and the peptide-to-lipid ratio.

Alamethicin adopts transmembrane alignments also in POPC lipid bilayers under conditions where zervamicin exhibits predominately in-plane orientations (Figures 5 and 6). Alamethicin is four amino acids longer than zervamicin, yielding an α -helix longer by approximately 6 Å. In addition, the side chains of the hydrophobic N-terminal residues can extend the hydrophobic length of alamethicin, whereas tryptophan, also present in zervamicin II, has been shown to act as an interfacial anchoring residue (58–60). Although structural analysis in methanolic solution (7, 61), and in the presence of SDS micelles (8, 9), identifies a flexible hinge region due to the helix-breaking motif G-X-X-P close to proline-14, X-ray structural analysis (6) and molecular dynamics in POPC bilayers suggest that the alamethicin helix

may adopt more extended conformations in phospholipid bilayers (12, 13). In zervamicin II three (hydroxy)proline residues are clustered at the C-terminal half of the peptide, whereas only the G-X-X-P motif involving proline-14 of alamethicin seems to strongly affect the H-bonding pattern and, therefore, the overall shape of the molecule. Although the length of the alamethicin helix might still be shorter than the hydrophobic thickness of an undisturbed POPC membrane, the difference seems to be sufficiently small to be compensated by adjustments of the bilayer thickness (42, 62, 63). In addition, the calculated hydrophobic moment of alamethicin and thereby the driving force to the membrane surface are less pronounced than in zervamicin (23). Considering the structures of zervamicin II and alamethicin, it is not surprising that alamethicin adopts more stable transmembrane alignments in POPC lipid bilayers and zervamicin II more in-plane alignments.

Topological equilibria have been observed with zervamicin (this study, Figure 6C), alamethicin (56, 57), large membrane proteins (64, 65), and hydrophobic and model sequences containing histidine and/or lysine side chains (42, 43, 54). Topological equilibria are important during insertion of large domains of membrane proteins (5) but also during the voltage-gating of small peptides such as the peptaibols (reviewed in refs 1–3 and 66). In the presence of phosphatidylcholine bilayers of a thickness commonly observed in biological membranes, zervamicin II orients parallel to the membrane surface (Figure 1A–C). Similarly in the absence of transmembrane potentials, in-plane alignments have been observed at high lipid-to-alamethicin ratios (57). It is believed that peptaibols are inactive in their in-plane orientation (27). Only by association as bundles of several transmembrane helices are electrophysiologically well-defined ion-conducting channels formed (25). Theoretical considerations indicate that transmembrane electric fields shift the in-plane to transmembrane equilibrium of a helix dipole by only a few kilojoules per mole (4). Therefore, a relatively small energetic difference should separate in-plane and transmembrane alignments in the absence of transmembrane potentials to enable the transmembrane electric field to exert detectable effects on the peptide orientations. Whereas the in-plane alignments of multiply charged amphipathic peptides seem to be stable due to excessive hydrophilic interaction contributions (4, 43), the present and previous studies indicate that in-plane to transmembrane transitions of peptaibols can be achieved by relatively small changes of sample composition. These include minor alterations of the hydrophobic thickness of the lipid bilayer (Figure 1), water activity (57), and, therefore, probably also transmembrane electric potentials (2). Interestingly the permeability of DOPC or egg PC vesicles is increased in the presence of peptaibols at L/P ratios similar to and higher than those used in this study even in the absence of transmembrane potentials (36, 67, 68). Our ^{15}N solid-state NMR data are consistent with alamethicin and zervamicin II exhibiting transmembrane helical alignments albeit in different proportions. Therefore, it remains possible that transmembrane helical bundle formation and pore formation occur also in the absence of voltage-gating. On the other hand, increases in membrane permeability induced by amphipathic peptide helices which exhibit stable in-plane alignments have also been observed (66). To explain these observations, various models, some of them based on

the detergent-like properties of amphiphiles, have been suggested (66). Detergent-like properties were also used as an explanation for the increased release of fluorescent dyes from large unilamellar vesicles at low L/P ratios and in the absence of transmembrane potentials (36, 69). The topological equilibria observed in the present study, however, are a prerequisite for models which involve helix reorientation of zervamicin II during voltage-gated channel formation.

ACKNOWLEDGMENT

We thank Cees Erkelens (Leiden Institute of Chemistry) for recording the 600 MHz NMR spectra, Kees Versluis (Bijvoet Center of Biomolecular Research, Utrecht University, The Netherlands) for measurement of the FAB MS spectra of [*Aib*₄/*S*⁻¹⁵N₄/*S*]zervamicin, Rudolf Kinder for technical help, and Natalia V. Swisheva (Shemyakin & Ovchinnikov Institute of Bioorganic Chemistry) and Tatjana Kropacheva (Chemistry Department, Udmurt State University, Izhevsk, Russian Federation) for HPLC purification of the samples.

REFERENCES

- Woolley, G. A., and Wallace, B. A. (1992) *J. Membr. Biol.* 129, 109–136.
- Sansom, M. S. (1993) *Eur. Biophys. J.* 22, 105–124.
- Cafiso, D. S. (1994) *Annu. Rev. Biophys. Biomol. Struct.* 23, 141–165.
- Bechinger, B. (1997) *J. Membr. Biol.* 156, 197–211.
- Bechinger, B. (2000) *Phys. Chem. Chem. Phys.* 2, 4569–4573.
- Fox, R. O., Jr., and Richards, F. M. (1982) *Nature* 300, 325–330.
- Yee, A. A., and O'Neil, J. D. (1992) *Biochemistry* 31, 3135–3143.
- Franklin, J. C., Ellena, J. F., Jayasinghe, S., Kelsh, L. P., and Cafiso, D. S. (1994) *Biochemistry* 33, 4036–4045.
- Spyracopoulos, L., Yee, A. A., and O'Neil, J. D. J. (1996) *J. Biomol. NMR* 7, 283–294.
- North, C. L., Franklin, J. C., Bryant, R. G., and Cafiso, D. S. (1994) *Biophys. J.* 67, 1861–1866.
- Yee, A. A., Marat, K., and O'Neil, J. D. J. (1997) *Eur. J. Biochem.* 243, 283–291.
- Tieleman, D. P., Sansom, M. S. P., and Berendsen, H. J. C. (1999) *Biophys. J.* 76, 40–49.
- Tieleman, D. P., Berendsen, H. J. C., and Sansom, M. S. P. (2001) *Biophys. J.* 80, 331–336.
- Vogel, H. (1987) *Biochemistry* 26, 4562–4572.
- Cascio, M., and Wallace, B. A. (1988) *Proteins* 4, 89–98.
- Brumfeld, V., and Miller, I. R. (1990) *Biochim. Biophys. Acta* 1024, 49–53.
- Barranger-Mathys, M., and Cafiso, D. S. (1996) *Biochemistry* 35, 498–505.
- Jayasinghe, S., Barranger-Mathys, M., Ellena, J. F., Franklin, C., and Cafiso, D. S. (1998) *Biophys. J.* 74, 3023–3030.
- Gordon, L. G., and Haydon, D. A. (1972) *Biochim. Biophys. Acta* 255, 1014–1018.
- Boheim, G. (1974) *J. Membr. Biol.* 19, 277–303.
- You, S., Peng, S., Lien, L., Breed, J., Sansom, M. S., and Woolley, G. A. (1996) *Biochemistry* 35, 6225–6232.
- Hanke, W., and Boheim, G. (1980) *Biochim. Biophys. Acta* 596, 456–462.
- Sansom, M. S. P. (1991) *Prog. Biophys. Mol. Biol.* 55, 139–235.
- Taylor, R. J., and de Levie, R. (1991) *Biophys. J.* 59, 873–879.
- La Rocca, P., Biggin, P. C., Tieleman, D. P., and Sansom, M. S. P. (1999) *Biochim. Biophys. Acta* 1462, 185–200.
- Kessel, A., Schulten, K., and Ben-Tal, N. (2000) *Biophys. J.* 79, 2322–2330.
- Huang, H. W. (2000) *Biochemistry* 39, 8347–8352.
- He, K., Ludtke, S. J., Heller, W. T., and Huang, H. W. (1996) *Biophys. J.* 71, 2669–2679.
- Breed, J., Kerr, I. D., Sankaramakrishnan, R., and Sansom, M. S. (1995) *Biopolymers* 35, 639–655.
- Schwarz, G., and Savko, P. (1982) *Biophys. J.* 39, 211–219.
- Stankowski, S., Schwarz, U. D., and Schwarz, G. (1988) *Biochim. Biophys. Acta* 941, 11–18.
- Duclohier, H. (2000) *J. Fluoresc.* 10, 127–134.
- Sansom, M. S. P., Balaran, P., and Karle, I. L. (1993) *Eur. Biophys. J.* 21, 369–383.
- Karle, I. L., Flippen-Anderson, J. L., Agarwalla, S., and Balaran, P. (1994) *Biopolymers* 34, 721–735.
- Balaran, P., Krishna, K., Sukumar, M., Mellor, I. R., and Sansom, M. S. (1992) *Eur. Biophys. J.* 21, 117–128.
- Kropacheva, T. N., and Raap, J. (1999) *FEBS Lett.* 460, 500–504.
- Karle, I. L., Flippen-Anderson, J. L., Agarwalla, S., and Balaran, P. (1991) *Proc. Natl. Acad. Sci. U.S.A.* 88, 5307–5311.
- Balashova, T. A., Shenkarev, Z. O., Tagaev, A. A., Ovchinnikova, T. V., Raap, J., and Arseniev, A. S. (2000) *FEBS Lett.* 466, 333–336.
- Bechinger, B., Kinder, R., Helmle, M., Vogt, T. B., Harzer, U., and Schinzel, S. (1999) *Biopolymers* 51, 174–190.
- North, C. L., Barranger-Mathys, M., and Cafiso, D. S. (1995) *Biophys. J.* 69, 2392–2397.
- Cross, T. A., and Quine, J. R. (2000) *Concepts Magn. Reson.* 12, 55–70.
- Harzer, U., and Bechinger, B. (2000) *Biochemistry* 39, 13106–13114.
- Vogt, T. C. B., Ducarme, P., Schinzel, S., Bresseur, R., and Bechinger, B. (2000) *Biophys. J.* 79, 2466–2656.
- Ogrel, A., Shvets, V. I., Kaptein, B., Broxterman, Q. B., and Raap, J. (2000) *Eur. J. Org. Chem.* 857–859.
- Egorova-Zachernyuk, T. A., Shvets, V. I., Versluis, K., Heerma, W., Creemers, A. F., Nieuwenhuis, S. A., Lugtenburg, J., and Raap, J. (1996) *J. Pept. Sci.* 2, 341–350.
- Ogrel, A., Bloemhoff, W., Lugtenburg, J., and Raap, J. (1997) *J. Pept. Sci.* 3, 193–208.
- Ogrel, A., Ogrel, S., Shvets, V., and Raap, J. (1998) *Let. Pept. Sci.* 5, 175–178.
- Bechinger, B., and Opella, S. J. (1991) *J. Magn. Reson.* 95, 585–588.
- Levitt, M. H., Suter, D., and Ernst, R. R. (1986) *J. Chem. Phys.* 84, 4243–4255.
- Rance, M., and Byrd, R. A. (1983) *J. Magn. Reson.* 52, 221–240.
- Valentine, K. G., Rockwell, A. L., Gierasch, L. M., and Opella, S. J. (1987) *J. Magn. Reson.* 73, 519–523.
- Witanowski, M., Stefanik, L., and Webb, G. A. (1986) *Annu. Rep. NMR Spectrosc.* 18, 2.
- Bechinger, B. (2000) *Mol. Membr. Biol.* 17, 135–142.
- Bechinger, B. (1996) *J. Mol. Biol.* 263, 768–775.
- Kessel, A., Cafiso, D. S., and Ben-Tal, N. (2000) *Biophys. J.* 78, 571–583.
- Huang, H. W., and Wu, Y. (1991) *Biophys. J.* 60, 1079–1087.
- Heller, W. T., He, K., Ludtke, S. J., Harroun, T. A., and Huang, H. W. (1997) *Biophys. J.* 73, 239–244.
- de Planque, M. R. R., Kruijtzter, J. A. W., Liskamp, R. M. J., Marsh, D., Greathouse, D. V., Koeppe, R. E., De Kruijff, B., and Killian, J. A. (1999) *J. Biol. Chem.* 274, 20839–20846.
- von Heijne, G. (1996) *Prog. Biophys. Mol. Biol.* 66, 113–139.
- Yau, W. M., Wimley, W. C., Gawrisch, K., and White, S. H. (1998) *Biochemistry* 37, 14713–14718.
- Yee, A., Szymczyna, B., and O'Neil, J. D. (1999) *Biochemistry* 38, 6489–6498.
- Lewis, J. R., and Cafiso, D. S. (1999) *Biochemistry* 38, 5932–5938.
- de Planque, M. R., Greathouse, D. V., Koeppe, R. E., Schafer, H., Marsh, D., and Killian, J. A. (1998) *Biochemistry* 37, 9333–9345.
- Kienker, P. K., Qiu, X., Slatin, S. L., Finkelstein, A., and Jakes, K. S. (1997) *J. Membr. Biol.* 157, 27–37.

65. Malenbaum, S. E., Merrill, A. R., and London, E. (1998) *J. Nat. Toxins* 7, 269–290.
66. Bechinger, B. (1999) *Biochim. Biophys. Acta* 1462, 157–183.
67. Beven, L., Duval, D., Rebuffat, S., Riddell, F. G., Bodo, B., and Wroblewski, H. (1998) *Biochim. Biophys. Acta* 1372, 78–90.
68. Dathe, M., Kaduk, C., Tachikawa, E., Melzig, M. F., Wenschuh, H., and Bienert, M. (1998) *Biochim. Biophys. Acta* 1370, 175–183.
69. Snook, C. F., Woolley, G. A., Oliva, G., Patabhi, V., Wood, S. F., Blundell, T. L., and Wallace, B. A. (1998) *Structure (London)* 6, 783–792.
70. Killian, J. A. (1998) *Biochim. Biophys. Acta* 1376, 401–416.
71. O'Brien, F. E. M. (1948) *J. Sci. Instrum.* 25, 73–76.
72. Zhang, Y. P., Lewis, R. N., Hodges, R. S., and McElhaney, R. N. (1992) *Biochemistry* 31, 11572–11578.

BI010162N